Pharmaceutical Research, Vol. 22, No. 5, May 2005 (© 2005)
DOI: 10.1007/s11095-005-2593-8

Research Paper

Effect of Particle Size of Nanospheres and Microspheres on the Cellular-Association and Cytotoxicity of Paclitaxel in 4T1 Cells

Sinjan De,[1] Donald W. Miller,[2] and Dennis H. Robinson[2,3]

Received August 5, 2004; accepted February 4, 2005

Purpose. To compare the effect of size of delivery systems on the cell-association and *in vitro* cytotoxicity of paclitaxel.
Methods. Four sizes of PLGA-paclitaxel particles were prepared to study the effect of particle size on the cell-association of paclitaxel in 4T1 monolayer in the presence, and absence, of BCRP inhibitor, endocytic inhibitor, and P-glycoprotein (P-gp) inhibitor. Paclitaxel cell-association studies were repeated in Caco-2, Cor-L23/R, and bovine brain microvessel endothelial cells (BBMECs), as well as the association of etoposide in 4T1 cells. Cytotoxicity of paclitaxel to 4T1 cells delivered in nanospheres was compared to microspheres.
Results. The concentration of paclitaxel and etoposide associated with 4T1 cells was 4.8 and 29 times greater, respectively, as the size increased from 310 to 2077 nm. Paclitaxel association consistently increased in Caco-2 and Cor-L23/R as the size of the delivery system increased. The endocytic inhibitor, 2-deoxyglucose, significantly decreased the cellular paclitaxel association when delivered by nanospheres but not microspheres. Consistent with the cell-association results, paclitaxel was thrice more cytotoxic to 4T1 cells when delivered in microspheres.
Conclusions. Cell-association of paclitaxel increased in 4T1, Caco-2, and Cor-L23/R as particle size increased. Paclitaxel delivered from 1-μm microspheres was thrice more cytotoxic to 4T1 cells compared to the drug delivered from nanospheres or solution.

KEY WORDS: cell-association; cytotoxicity; microsphere; nanosphere; paclitaxel.

INTRODUCTION

Breast cancer is the second leading cause of cancer-related deaths in women. Worldwide, the incidence of breast cancer is 100.6 cases per 100,000 women, and the American Cancer Society expects more than 215,990 women in the United States would be diagnosed with the disease in 2004, and 40,110 deaths are expected (1).

Paclitaxel is a potent drug used to treat breast and ovarian cancer, and the National Cancer Institute considers this drug as the most significant advance in chemotherapy in the past 15 years. This drug prevents division of cancer cells by stabilizing the mitotic spindle and inhibiting daughter cell separation, thereby causing toxicity and eventually, cell death (2,3). The recommended dose of paclitaxel, 175 mg/m^2 of body surface area, is administered via intravenous infusion over 24 h, every 21 days (4–7). A major problem of paclitaxel is its low aqueous solubility (less than 1 μg/ml) (8). The commercially available formulation uses a 1:1 cosolvent mixture of ethanol and Cremophor EL (polyethoxylated castor oil) (6,8). However, Cremophor EL is biologically and pharmaceutically active, causing anaphylactic hypersensitivity, hyperlipidemia, neurotoxicity, and *in vitro* cytotoxicity due to the formation of free radicals (9,10). In attempts to overcome the low aqueous solubility of paclitaxel as well as the undesirable toxicity of Cremophor EL, numerous alternate dosage forms have been investigated including gels (11), films (12), emulsions (13–15), liposomes (16–18), macromolecule conjugates (19), and particulate delivery systems (20–32).

Nanospheres and microspheres containing paclitaxel have been investigated using various polymers such as poly-lactic-*co*-glycolic acid (PLGA) (21,30–33), poly-lactic acid (24,25), poly-ethylene oxide (25,26,31), poly-propylene oxide (27), and poly(ε-caprolactone) (20). The proposed advantages of particulate delivery systems for paclitaxel are that they 1) may avoid the use of toxic polyethoxylated castor oil, 2) may evade cellular efflux pumps, 3) can be administered orally or systemically, 4) inhibit tumor growth as well as prevent relapse after surgery, and 5) sustain the release of paclitaxel at therapeutic concentrations. For these reasons, it was proposed that paclitaxel delivered in a particulate formulation would be safer and more cytotoxic to tumor cells than an intravenous solution. In addition, a sustained-release particulate delivery system of paclitaxel would decrease dosing frequency. The release of the paclitaxel from the PLGA particles is reported to be slow, for example, 55% in 60 days from nanospheres (33) and 40% in 105 days from microspheres (34). Hence, a faster and more complete release of paclitaxel is essential. To accelerate the release of paclitaxel, surfactants

[1] College of Pharmacy, Ohio Northern University, Ada, Ohio, USA.
[2] Department of Pharmaceutical Sciences, College of Pharmacy, University of Nebraska Medical Center, 98605 Nebraska Medical Center, Omaha, Nebraska 68198-6025, USA.
[3] To whom correspondence should be addressed. (e-mail: dhrobins@unmc.edu)

such as polyvinyl alcohol, vitamin E, and dipalmitoyl phosphatidylcholine have been added to reduce the surface tension and solubilize the hydrophobic drug (18–30,32–35). Although, there has been significant progress in the development of particulate delivery systems containing paclitaxel, the effect of particle size of the nanospheres and microspheres preparation on the extent and mechanism of cell-association and cytotoxicity into the cancer cells has not been thoroughly investigated.

The extent of internalization of particles into cells has been reported to be inversely proportional to the particle size range (36–38). Particles and droplets less than 100 nm can enter cells by pinocytosis (fluid-phased endocytosis) that occurs when an endosome containing fluid is formed by invagination of the plasma membrane. Particles within the size range of 100 nm and 5 μm are internalized by endocytosis when the cell bilayer invaginates to encapsulate the particles within a vesicle called the endosome. These endosomes fuse with lysosome to form an endo-lysosome that degrades foreign materials because of their acidic environment and lysosomal enzymes. However, nanospheres evade lysosomal degradation by a proton-sponge effect that inhibits the formation of an acidic pH environment inside the lysosome, and as a result are released from the endolysosome into the cytoplasm (39). Therefore, the paclitaxel entrapped within the nanospheres or microspheres may evade lysosomal degradation and slowly release the drug inside the cell. This research investigates the mechanism of the cell-association of paclitaxel delivered in PLGA particles of varying size into, or onto, 4T1 cells. In addition, this research compares the cell-association of paclitaxel in 4T1 cells with other cell lines such as, Caco-2, Cor-L23/R, and bovine brain microvessel endothelial cells (BBMECs). Further, to determine if the drug entrapped inside various particulate PLGA formulations affects cellular association, the internalization of nanospheres and microspheres into 4T1 cells was also investigated with another anticancer drug, etoposide. The overall objective of this research was to compare the effect of particle size of nanospheres and microspheres on the extent of drug cell-association and *in vitro* cytotoxicity of paclitaxel, primarily in the highly metastatic, aggressive, murine, 4T1 breast cancer cells.

The specific aims of this research were 1) to study the effect of particle size of PLGA nanospheres and microspheres on the extent of cellular association of paclitaxel into or onto 4T1 and other cells; 2) to identify and compare the mechanism(s) of absorption of paclitaxel into cells, when delivered from nanospheres and microspheres of varying size; and 3) to study the effect of particle size of PLGA nanospheres and microspheres on the cytotoxicity of paclitaxel in 4T1 cells.

MATERIALS AND METHODS

Materials

Polylactic-*co*-glycolic acid (PLGA) (50:50) with inherent viscosity of 0.69 dl/g was obtained from Birmingham Polymers Inc. (Birmingham, AL, USA). Paclitaxel, polyvinylalcohol (PVA), sodium chloride, sodium dihydrogen phosphate, disodium hydrogen phosphate, acetonitrile, methanol, dimethyl sulfoxide (DMSO), phenylarsine oxide, 2-deoxyglucose (2-DG), potassium cyanide, carbachol, etoposide, and lucifer yellow were purchased from Sigma Chemical (St. Louis, MO, USA). Dichloromethane was obtained from Aldrich Chemical Co. Inc. (Milwaukee, WI, USA).

Iscove's Dulbecco's modified Eagle medium, trypsin-EDTA, heat-inactivated fetal bovine serum, and antibiotic/antimycotic solutions were obtained from Gibco, Invitrogen Corporation (Grand Island, NY, USA). Fumitremorgin-C was kindly donated by Dr. Robert J. Schultz at the National Cancer Institute (Bethesda, MD, USA). Caco-2 and Cor-L23/R were obtained from ATCC (Manassas, VA, USA). 4T1 cells were kindly donated by Dr. Donald Miller, Nebraska Medical Center (Omaha, NE, USA). BBMEC cells were primary cultures isolated by Miller *et al.* from bovine brain.

Methods

Preparation of Paclitaxel Nanospheres and Microspheres of Varying Size

Nanospheres and microspheres of varying size were prepared by altering the method of agitation used during the solvent evaporation method. Paclitaxel (2 mg) was dissolved in 3 ml of PLGA solution (30 mg/ml) in dichloromethane and then emulsified with 25 ml of 1.5% w/v aqueous polyvinyl alcohol saturated with dichloromethane. Nanospheres with mean diameters of approximately 310 and 456 nm were produced by sonicating (using Misonix Sonicator 3000, Farmingdale, NY, USA) the dispersion for 60 s at 36 and 10 W, respectively. Similarly, microspheres of 1 and 2 μm in diameter were formed when the dispersion was emulsified using a Sorvall Omni-mixer (Norwalk, CT, USA) for 60 s at 3 W and 1 W, respectively. The dichloromethane was evaporated from the emulsion by slowly agitating overnight with a magnetic stirrer, and the particles were centrifuged then washed twice with distilled water at 140,000 × *g* for 20 min. The resultant pellet was resuspended in water, lyophilized, and stored at 4°C until required.

Diameter and Morphology of PLGA Nanospheres and Microspheres Containing Paclitaxel

The mean particle size and zeta-potential of each batch of nanospheres and microspheres was analyzed by dispersing 0.5 mg samples in 3 ml of water using dynamic light scattering (Zeta Plus particle size analyzer, Brookhaven Instrument Corporation, Holtsville, NY, USA). Scanning electron microscopy (SEM) was used to confirm size and study surface morphology of the particles (0.5 mg) after coating with chromium under vacuum at 95 mA and visualized using 5 kV and the digital images recorded.

Release of Paclitaxel from PLGA Nanospheres and Microspheres

An *in vitro* differential dissolution method was used to study the effect of size of paclitaxel-PLGA particles (310, 456, 1040, and 2077 nm) on drug release. The particles (equivalent to 30 μg of paclitaxel per sample) were suspended in 25 ml of the dissolution media consisting of 0.1% v/v aqueous Tween 80 to maintain sink conditions and incubated at 37°C while shaking at 50 rpm in a shaking water bath. To monitor the amount of drug released at selected time intervals, samples were centrifuged at 140,000 × *g* for 20 min at 4°C and the

supernatant lyophilized. The dissolution study was continued by resuspending the pellet in 25 ml of fresh buffer and the process repeated at each time interval. The paclitaxel concentration was determined using high-performance liquid chromatography (HPLC) after dissolving the lyophilized powder in 1 ml of acetonitrile for 16 h at 37°C. The results of paclitaxel release was statistically analyzed within groups for standard error and between groups using Student's *t* test at $\alpha = 0.05$.

Association of Drugs with 4T1 and Other Cell Lines

The 4T1 murine epithelial breast cancer cell line was used for most cell-association and cytotoxicity studies involving paclitaxel. In addition, the effect of paclitaxel cell-association from various sized particles was investigated in epithelial human colon cancer (Caco-2) and epithelial human large lung cancer (Cor-L23/R) cells as well as in primary cultured bovine brain microvessel endothelial cells (BBMECs). The cellular association of the paclitaxel included not only the internalized drug and particles but also any particles that might have adhered to the surface of the cells, not removed by normal washing procedure. The following media were used: Iscove's modified DMEM medium, DMEM, RPMI 1640, and MEM Ham's F12 for 4T1, Caco-2, Cor-L23/R, and BBMECs, respectively. To study the cell-association of paclitaxel, the cells were seeded on 6-well plates (seeding density of 4T1, 22,222 cells/cm^2; Caco-2, 27,778 cells/cm^2; Cor-L23/R, 4444 cells/cm^2; BBMECs, 33,333 cells/cm^2) and cultured to confluency (4T1, 3 days; Caco-2, 10 days; Cor-L23/R, 8 days; and BBMECs, 12 days) at 37°C in a humidified atmosphere with 5% v/v CO_2.

To examine cellular association of drug, the growth media was removed and the cell monolayer pretreated with 1 ml of assay buffer that included Iscove's modified Eagle medium containing pretreatment agent, if needed, (e.g., endocytic or efflux transport inhibitor), for 30 min at 37°C. Following pretreatment, the cells were exposed to Iscove's modified Eagle media containing 35 μM paclitaxel (30 μg) in each well either in solution or as a suspension of nanoparticles or microparticles. After the cells were incubated for 90 min, the medium was removed, and the monolayers washed three times with 1 ml PBS at 4°C, then incubated with additional 1 ml of PBS at 37°C for 30 min while shaking at 50 rpm. The PBS wash removed lightly bound particles from the cellular surface or particles present in the suspension. Therefore, the cells now contained internalized drug, particles and also particles that might be adhered to the surface. The cells were detached from the wells using a cell scraper and transferred to a 1.5 ml Eppendorf tube, lyzed by sonicating for 15 s at 6 W, and three cycles of freeze thawing. Aliquots (25 μl) were removed to determine total cell protein using a BCA protein assay kit. To determine the amount of cell-associated paclitaxel, cell lysates were lyophilized to concentrate the sample, and the drug (free and particle associated) extracted with acetonitrile. The paclitaxel concentration was determined using HPLC. The results of paclitaxel cellular association was statistically analyzed within groups for standard error and between groups using Student's *t* test at $\alpha = 0.05$.

Cellular Association of Lucifer Yellow into 4T1 Monolayers in Presence of Endocytic Inhibitors

To determine if endocytosis was the mechanism of drug association, the influence of several endocytic inhibitors on the accumulation of a fluorescent, pinocytotic marker, lucifer yellow, into 4T1 monolayers was studied. This protocol was similar to that used to study the association of paclitaxel into 4T1 monolayers described above. However, the cells were incubated with 1 ml of 1000 μM aqueous lucifer yellow rather than paclitaxel solution and the fluorescent marker was analyzed spectrofluorometrically (λ_{ex} 430 nm and λ_{em} 540 nm). The endocytic inhibitors tested for optimal inhibition were 2-deoxyglucose (50 mM), potassium cyanide (1 mM), or carbachol (300 μM) and were added separately to the 6-well plates in the assay buffer during pretreatment and in media during treatment with lucifer yellow. The results of inhibition of cellular association of lucifer yellow was statistically analyzed within groups for standard error and statistical significance between the inhibitor groups and solution control was determined using Student's *t* test at $\alpha = 0.05$.

Association of Paclitaxel into 4T1 Cells in the Presence of Endocytic and P-glycoprotein Inhibitors

From the above experiment, 2-deoxyglucose (2-DG) was most effective in inhibiting endocytosis and, hence, the association of paclitaxel into 4T1 cells was investigated in presence of 50 mM 2-deoxyglucose in water. In this study, 2-deoxyglucose was added during the pretreatment and treatment stages, to the assay buffer and media (in combination with paclitaxel), respectively. The particle size-dependent association of paclitaxel into 4T1 cells was also repeated in presence of a specific breast cancer resistance protein (BCRP) inhibitor, fumitremorgin-C (FTC, 5 μM in methanol) to investigate the role of efflux pump in the particle size–dependent cellular association of paclitaxel. In BBMEC monolayers, the association was repeated in presence of a P-glycoprotein inhibitor, cyclosporin A (2 μg/ml). Inhibition of BCRP or P-gp efflux pump by FTC or cyclosporin A, respectively, should increase the intracellular concentration of the drug.

Treatment of Cell Surface After Incubation with PLGA Particles

To differentiate between specific receptor binding of PLGA nanospheres and microspheres to the surface of the cells or nonspecific surface adhesion, the particle size–dependent association of paclitaxel into 4T1 monolayers was repeated after an additional acid washing step to remove particles bound to specific protein sites on the membrane. The 4T1 monolayers were washed with 1.0 ml of a 50:50 aqueous mixture of 0.2 M acetic acid and 0.5 M NaCl (pH 3.0) after incubation with either the paclitaxel solution or a suspension of particles of four varying sizes. The plates were then incubated at 4°C for 6 min, media removed, and the cells washed, detached, and lyzed. The paclitaxel concentration was again determined by HPLC. The standard error of paclitaxel cellular association was determined within the acid and untreated groups. The statistical significance between the acid treated and untreated groups were tested using Student's *t* test at $\alpha = 0.05$.

Confocal Visualization of the Particle Size–Dependent Association of PLGA Particles Containing The Fluorescent Dye, BODIPY, into 4T1 monolayers

PLGA particles were prepared using the fluorescent dye BODIPY using an emulsification evaporation method. The lipophilic fluorescent dye, BODIPY, mimics paclitaxel and the release can be visually observed using confocal microscopy. The sizes of the BODIPY-PLGA particles used for this study were 266.9 ± 2.8, 541.6 ± 1.8, 988.8 ± 14.1, and 1865.9 ± 67.0 nm, respectively. The 4T1 cells were seeded onto 4 BIOPTECH plates (75,000 cells/ml per plate) and after incubation for 16 h in a humidified atmosphere of 5% v/v CO_2 resulted in 60% cellular confluency. The medium was replaced with 1 ml of assay buffer, and after 30 min, the assay buffer was replaced with 1 ml of a specific size of nanoparticle or microparticle suspension (approximately 250 μg/ml) to the plates. After incubation in a humidified atmosphere of 5% v/v CO_2 at 37°C for various times (90 min to 141 h), the particles were removed and the cells washed thrice with 1 ml of ice-cold PBS. The PBS was then replaced with 1 ml of ice-cold assay buffer and the cell associated fluorescence (λ_{ex} = 505 nm and λ_{em} = 511 nm) observed using confocal microscopy, with a filter of 488 nm and cutoff filter at 515 nm.

Cellular Association of Etoposide When Delivered from Nanospheres and Microspheres

To establish if the increase in the amount of paclitaxel associated with 4T1 monolayers when delivered in PLGA microspheres was a property of the delivery system rather than the drug, the cellular association (both internalized and surface associated) study was repeated under identical conditions using PLGA nanospheres and microspheres in similar sizes used previously, containing etoposide. Although, sparingly soluble in water (141–200 μg/ml, 25°C), etoposide is more hydrophilic than paclitaxel (40). The same emulsion method was used to prepare etoposide-PLGA particles with mean diameter of 299, 410, 1120, and 1890 nm. Drug loading of etoposide for the batches with increasing sizes were 0.17%, 0.23%, 0.54%, and 0.55% w/w, respectively. The standard error of etoposide cellular association was determined within groups. The statistical significance between the different sized particles were tested using Student's *t* test at $\alpha = 0.05$.

Cytotoxicity Studies with Paclitaxel-PLGA Particles

The 4T1 cells were seeded (5000 cells/well) onto 96-well plates in Iscove's modified Dulbecco's media supplemented with 1% v/v antibiotic/antimycotic solution and 10% v/v heat-inactivated fetal bovine serum. The cells were incubated for 16 h at 37°C in a humidified atmosphere of 5% v/v CO_2, then washed and the media replaced with either 100 μl of paclitaxel solution or 100 μl of a suspension containing paclitaxel-PLGA particles with sizes of 309, 450, 1040, or 2077 nm, in antibiotic-free media. Varying concentrations of paclitaxel (0, 0.1, 0.32, 0.64, 1, 3.2, 6.4, 10, 32, and 100 μM), either as solution or particulate suspension, were obtained by appropriate dilution of a 1 mM stock solution in DMSO. After incubation for 8 h at 37°C in humidified 5% CO_2 v/v, the media was removed and the cells washed with 100 μl of fresh, antibiotic-free media. This washing medium was again replaced with 200 μl of antibiotic-free media and the cells incubated at 37°C for an additional 72 h in a humidified atmosphere of 5% v/v CO_2. Viable cells were measured using the MTT (methylthiazolyldiphenyl tetrazolium bromide) assay (41,42). Briefly, the media was removed and the cells incubated for 2 h with 100 μl of fresh media and 25 μl of MTT reagent (5 mg/ml). After 2 h, 100 μl of a solvent consisting of 20% w/v sodium dodecyl sulfate in 1:1 dimethylformamide:water, pH 4.7, was added to the wells and incubated for 10 h. An ELISA plate reader was used to determine the optical density of the contents in each well at 550 nm that is directly proportional to cell viability. The IC_{50} of paclitaxel delivered from the particles of varying size was generated from the cytotoxicity profiles using the dose-response, nonlinear regression curve software, GraphPad Prism version 3.02 for Windows (GraphPad Software, San Diego, CA, USA). To confirm that DMSO did not interfere with cell viability, the cytotoxicity experiments were repeated, without paclitaxel in solution or PLGA particles, while using concentrations of DMSO identical to the above protocol namely, 0%, 0.01%, 0.032%, 0.064%, 0.1%, 0.32%, 0.64%, 1%, and 3.2% v/v.

HPLC Analyses of Paclitaxel and Etoposide

Paclitaxel was analyzed by a method modified from Shao and Locke, using a HPLC (Shimadzu, SIL 9A, Columbia, MD, USA) fitted with a C_{18} column (Curosil PFP, 250 × 60 mm, 5 μm, Phenomenex, Torrance, CA, USA) and a mobile phase of 60:40 v/v mixture of acetonitrile and water adjusted to pH 4.0 with 0.1 M HCl (43). The flow rate was 1 ml/min and paclitaxel in acetonitrile (10 μl) monitored at 237 nm (Shimadzu, SPD-6AV detector). Paclitaxel eluted after 6.2 min and was quantified from a calibration graph of solutions of paclitaxel in acetonitrile in the concentration range between 0 to 6 μg/ml.

The concentration of etoposide was determined using the method developed by Shah *et al.* (44). The mobile phase consisted of a mixture of 72:0.75:27.25 water adjusted to pH 5.0 with 0.1 M HCl, acetic acid, and acetonitrile. Using a C_{18} column (Curosil PFP, 250 × 60 mm, 5 μm, Phenomenex) and a flow rate of 1.5 ml/min, and etoposide (retention time of 7.7 min) was quantified at 230 nm. The etoposide concentrations in the samples were quantified from the HPLC calibration graph of the drug solution in acetonitrile between concentration ranges of 0 to 10 μg/ml.

RESULTS AND DISCUSSION

Characterization of Paclitaxel-PLGA Nanospheres and Microspheres

The particle diameters ± SE were 310 ± 18, 450 ± 7, 1040 ± 30, and 2077 ± 102 nm (Table I) (45–47). The loading efficiencies of paclitaxel within the particles were independent of

Table I. Increase in Dissolution Half-Life of Paclitaxel as a Function of Particle Size

Particle size (nm)	Dissolution half-life (h)	Loading efficiency (%)
310 ± 18	1.5	80.1 ± 2.6
450 ± 7	3	80.2 ± 2.0
1040 ± 30	55	84.2 ± 1.4
2077 ± 102	130	82.5 ± 3.6

Mean ± SE.

size and were 80.1 ± 2.6, 80.2 ± 2.0, 84.2 ± 1.4, and 82.5 ± 3.6% w/w, respectively (Table I). SEM revealed that some crystalline needles of paclitaxel, 300–900 nm in length, adhered to the surface of the nanospheres, particularly the 310-nm samples. These drug crystals were not observed in microspheres. Despite altering formulation parameters such as, PVA concentration, volume of dichloromethane, and addition of organic cosolvents, formation of these crystals could not be eliminated or removed. The presence of paclitaxel on the surface of the nanospheres may be due to precipitation of the drug as the dichloromethane evaporated during manufacture resulting in incomplete entrapment of drug. Importantly, free paclitaxel crystals were not observed on microsphere preparations (1040- and 2077-nm microspheres).

Release of Paclitaxel from the Paclitaxel-PLGA Nanospheres and Microspheres

Due to the decrease in surface area to mass ratio, the rate of release of paclitaxel decreased as particle size increased (Fig. 1). Whereas smallest nanospheres (310 nm) released almost 100% of paclitaxel in less than 30 h, only 70% was released from 2 μm microspheres after 500 h. The dissolution half lives increased from 1.5 h for 310 nm nanospheres to 130 h for 2077 nm microspheres (Table I).

Influence of Particle Size on the Amount of Paclitaxel Associated with 4T1 Monolayers

The amount of cell-associated paclitaxel consistently increased as particle size increased (Fig. 2). The drug analyzed from the experiment was expected to come from three different sources: i) internalized paclitaxel, ii) drug associated with the internalized particles, iii) drug associated with the particles adhered to the cellular surface.

The amount of cell-associated paclitaxel delivered by the largest microsphere was 4.8 times greater than the 309 nm nanospheres and 7 times greater than the solution (Fig. 2). As the cell-association of paclitaxel from solution was similar in the presence or absence of PLGA placebo particles, it was concluded that the polymer did not influence the extent of drug association. The observation that the amount of drug associated with 4T1 cells increased as the particle size increased, is contrary to previous reports (36–38). The two explanations for the observation that the amount of paclitaxel associated with 4T1 cells was greater when delivered in microspheres than nanospheres are: First, efflux pumps such as p-glycoprotein (P-gp) or breast cancer resistant protein (BCRP) present within the cell membrane may eliminate the internalized paclitaxel. Although paclitaxel is a substrate for P-gp (48,49), this efflux pump is absent in 4T1 cells. However, as BCRP may be present, the cell-association of paclitaxel from solution or nanospheres will increase in the presence of a specific BCRP inhibitor, such as fumitremorgin-C (fungal mycotoxin) (50,52). Second, internalization of paclitaxel increased because microspheres adhered to the surface of epithelial cells, thus facilitating an increased cell-surface–association of drug that later internalized (53). It is known that nanospheres can enter the cells by endocytosis (36–38), although, the internalization of microspheres is unknown (54). To determine if microspheres were endocytosed, the cell-association of paclitaxel was repeated in the presence of the endocytic inhibitor, 2-DG (55). If microspheres were not internalized, the increase in the amount of cellular paclitaxel may be explained by the sustained, localized release of drug from particles adhering to the cellular surface. The following series of experiments were designed to explain why the association of paclitaxel onto or into 4T1 cells increased as the particle size of the delivery system increased. Further, surface association and accumulation of PLGA particles of varying sizes were studied using confocal microscopy.

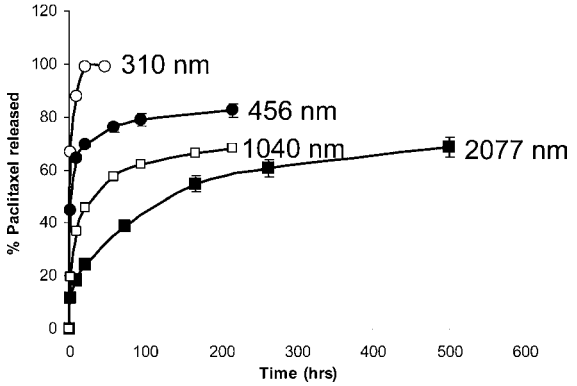

Fig. 1. The release of paclitaxel from PLGA nanospheres and microspheres. Mean ± SE.

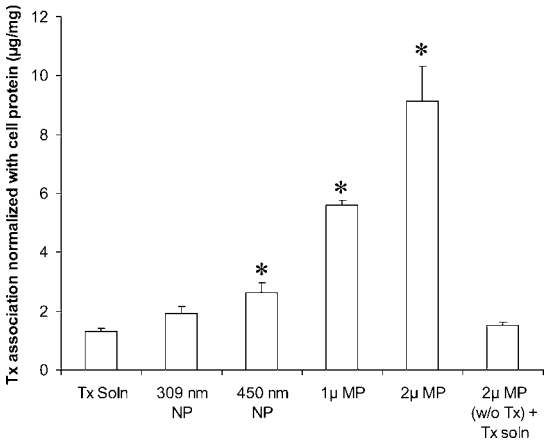

Fig. 2. Concentration of paclitaxel associated with 4T1 cells as a function of particle size of the delivery system. Tx = paclitaxel, Tx soln = paclitaxel solution, 309 nm NP = nanospheres of size 309 nm, 450 nm NP = nanospheres of size 450 nm, 1μ MP = microspheres of size 1 μm, 2μ MP = microspheres of size 2 μm. (*Indicates statistically significant at $\alpha = 0.05$.) Mean ± SE.

Effect of Drug Efflux Transporters on the Association of Paclitaxel into 4T1 Monolayers

There was no statistical significant difference ($p = 0.113$) in the amount of paclitaxel internalized within 4T1 cells in the absence or presence of 5 μM FTC (51,52). The mean and standard error of the amount internalized was 1.524 ± 0.006 and 1.244 ± 0.200 μg per mg of cell protein, respectively. Hence, it was concluded that BCRP was either absent from the surface of 4T1 cells or does not inhibit the association of paclitaxel from solution.

Identification of a Suitable Endocytic Inhibitor

Figure 3 illustrates that the cell-association of lucifer yellow decreased with each of 2-deoxyglucose (50 mM), potas-

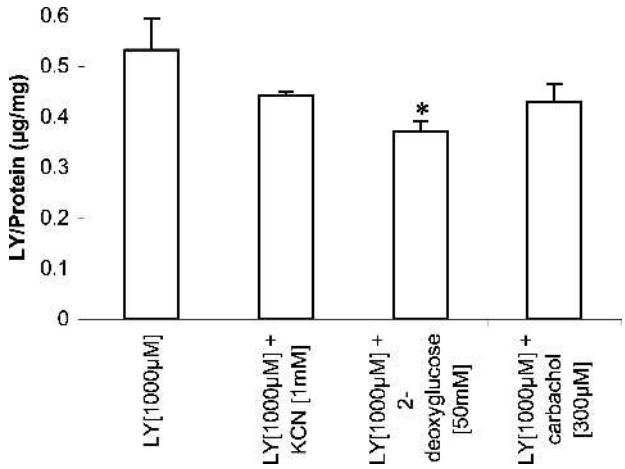

Fig. 3. Inhibition of lucifer yellow cell-association in presence of selected endocytic inhibitors, potassium cyanide, 2-DG, and carbachol. LY = lucifer yellow. (*Indicates statistically significant at $\alpha = 0.05$.) Mean ± SE.

sium cyanide (1 mM), and carbachol (300 µM) (56). Of the three inhibitors, only the inhibition by 2-deoxyglucose was statistically significant at $\alpha = 0.05$. Hence, 2-deoxyglucose was used in subsequent experiments to evaluate the effect of an endocytic inhibitor on paclitaxel cell-association.

The Cell-Association of Paclitaxel in the Presence of the Endocytic Inhibitor, 2-Deoxyglucose

In the presence of 2-DG, the concentration of cell-associated paclitaxel significantly decreased in 4T1 cells in the 309 nm, 450 nm, and 1 µm particulate formulations. In contrast despite variation in results, the endocytic inhibitor had no effect on cell-associated paclitaxel in the 2.0-µm microspheres (statistical significance was 0.071) (Fig. 4). This experiment was repeated several times, and 2-DG did not demonstrate any statistical significance in the paclitaxel cell-association from the 2.0-µm microspheres. Further, despite the presence of 2-DG, the magnitude of cell-association increased with increasing particle size. As expected, 2-DG did not affect the pinocytotic cell-association of paclitaxel from solution into 4T1 monolayers. These data indicate that both endocytosis and cell-adhesion simultaneously takes place from all sizes of particles, however the association of paclitaxel delivered from the nanospheres is predominantly by endocytosis. Therefore, although cell-association of particles by endocytosis decreases as the size increases, the amount of paclitaxel in or around the cells increases (Fig. 4). This suggests that paclitaxel associated from microspheres is predominantly by adhesion of particles to the surface of the cells and minimally through endocytosis from the smaller particle fractions.

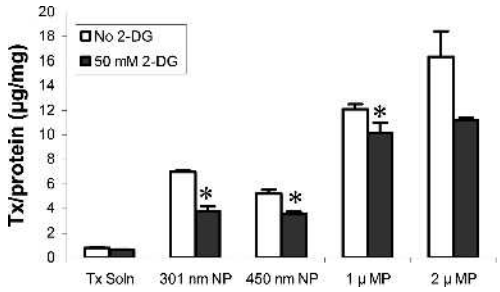

Fig. 4. The effect of particle size of delivery system on association of paclitaxel into 4T1 monolayers in presence of 50 mM endocytic inhibitor, 2-deoxyglucose. Tx = paclitaxel, Tx soln = paclitaxel solution, 309 nm NP = nanospheres of size 309 nm, 450 nm NP = nanospheres of size 450 nm, 1µ MP = microspheres of size 1 µm, 2µ MP = microspheres of size 2 µm. (*Indicates statistically significant at $\alpha = 0.05$.) Mean ± SE.

Effect of Surface Treatment of 4T1 Monolayers on Drug Association After Incubation with Paclitaxel-PLGA Particles of Varying Size

As the surface treatment with 0.2 M acetic acid and 0.5 M NaCl (pH 3.0) did not significantly affect the association of paclitaxel delivered from the four sizes of particles (Fig. 5), it was concluded that binding of the microspheres to the 4T1 cell surface was nonspecific (57). However, the association of paclitaxel from the 309-nm nanospheres did show a significant decrease in the accumulation, but this was accounted to experimental variation and error.

Visualization of Particle Size–Dependent Association of BODIPY-PLGA Nanospheres and Microspheres into 4T1 Monolayer

Figures 6a and 6b illustrate that nanospheres (266 and 541 nm) were observed mainly inside the cytoplasm with a limited number in the nuclei and intercellular spaces (58). Conversely, the 1- and 2-µm microspheres adhered to the surface of the cells in addition to the intercellular spaces (Figs. 6c and 6d). The particles in the intercellular spaces are green, indicating they are at the same level of focus as the cells, while those on the cells appear gray and out of focus of the confocal microscope. Subsequent confocal layered imaging (z-sections) confirmed that the microspheres were associated with the surface of 4T1 cells.

Figure 7 illustrates that unlike other sizes, the 2-µm microspheres were adhered to the surface of the 4T1 cells. Further, the increase in intracellular concentration of BODIPY with time indicates that the dye is slowly released from the PLGA microspheres and then internalized into the cells. The

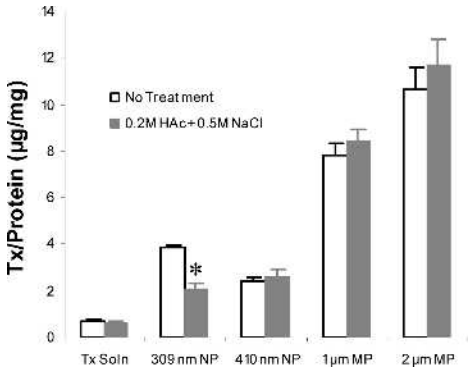

Fig. 5. Effect of surface treatment of 4T1 cells on association of paclitaxel delivered from nanospheres and microspheres. Tx = paclitaxel, Tx soln = paclitaxel solution, 309 nm NP = nanospheres of size 309 nm, 450 nm NP = nanospheres of size 450 nm, 1µ MP = microspheres of size 1 µm, 2µ MP = microspheres of size 2 µm, HAc = acetic acid. (*Indicates statistically significant at $\alpha = 0.05$.) Mean ± SE.

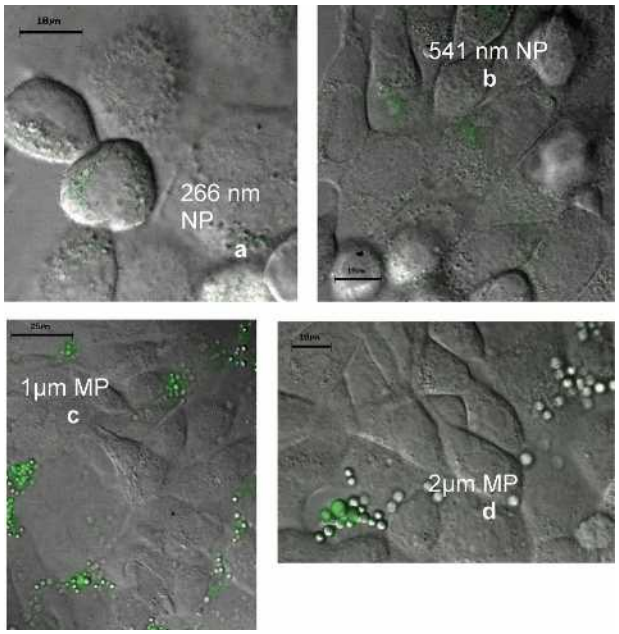

Fig. 6. Confocal photomicrographs illustrating the localization of fluorescent BODIPY-PLGA nanospheres and microspheres in 4T1 cells. 266 nm NP = nanospheres of size 266 nm, 541 nm NP = nanospheres of size 541 nm, 1μ MP = microspheres of size 1 μm, 2μ MP = microspheres of size 2 μm.

microspheres remained intact, nonaggregated, and highly fluorescent for the duration (141 h) of the experiment (Fig. 7).

Particle Size–Dependent Association of Etoposide into 4T1 Monolayers

Consistent with the data obtained with paclitaxel, the association of etoposide into 4T1 monolayers also increased as particle size increased (Fig. 8). The increase in intracellular concentration of etoposide delivered by the 2-μm microspheres was 20-fold greater than from the drug solution, and almost three times that observed for the largest paclitaxel microspheres. These data further suggest that the increase in intracellular concentration of anticancer agents in these cell

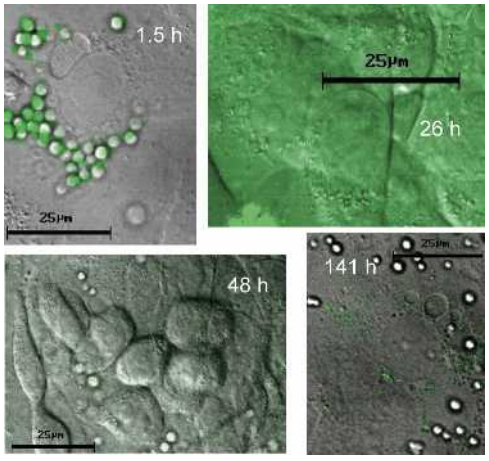

Fig. 7. Time-dependent increase of the association of BODIPY with the 4T1 monolayers delivered in 2-μm PLGA microspheres. h = hour.

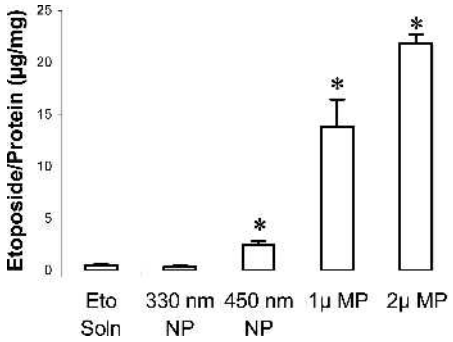

Fig. 8. Effect of particle size of nanospheres and microspheres on the concentration of etoposide association into the 4T1 cells. Tx soln = paclitaxel solution, 309 nm NP = nanospheres of size 309 nm, 450 nm NP = nanospheres of size 450 nm, 1μ MP = microspheres of size 1 μm, 2μ MP = microspheres of size 2 μm. (*Indicates statistically significant at $\alpha = 0.05$.) Mean ± SE.

lines observed with increasing size of the particles, was a property of the delivery system and independent of the drug.

Cell-Dependent Association of Paclitaxel from PLGA Particles

Table II summarizes the percentage increase in the association of paclitaxel into Caco-2, Cor-L23/R, and BBMECs as a function of the size of nanospheres and microspheres. Figure 9 illustrates that, consistent with observations in 4T1 cells, the association of paclitaxel in Caco-2 and Cor-L23/R cell monolayers increased as particle size increased. In contrast, there was no increase in paclitaxel association in noncancerous BBMECs with the particle preparations compared to cancerous cells. It is speculated that the high density of charge present on the surface of the endothelial cells can selectively reduce the cell-association of the negatively charged PLGA particles, as was observed in the case of BBMECs (59).

Effect of Cyclosporin A on the Particle Size–Dependent Association of Paclitaxel into BBMEC Monolayers

Paclitaxel is a substrate for P-gp and in the presence of the P-gp inhibitor, cyclosporin A, the intracellular association of the drug from solution increased due to the inhibition of the efflux pump. However, as the intracellular association of paclitaxel in BBMEC delivered from the 450-nm, 1-μm, and 2-μm particles did not significantly increase in the presence of cyclosporin A, it was concluded that the particulate delivery systems protect the drug from the effects of the P-gp efflux pump. The statistically significant increase in paclitaxel cell-

Table II. Association of Paclitaxel from Particles of Varying Sizes into Different Cell Lines

Paclitaxel delivery	% Paclitaxel association relative to solution			
	4T1	Caco-2	Cor-L23/R	BBMEC
Solution	100.00	100.00	100.00	100.00
301 nm NP[a]	143.70	68.27	45.51	57.49
410 nm NP[a]	197.05	107.03	346.10	298.01
1 μm MP	421.06	221.37	1365.02	168.18
2 μm MP	686.52	344.77	2309.99	87.53

[a] NP, nanoparticles.

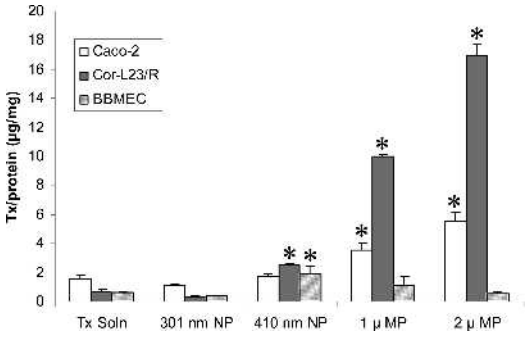

Fig. 9. Effect of particle size of nanospheres and microspheres on the concentration of paclitaxel association into Caco-2, Cor-L23/R, and BBMEC monolayers. Tx = paclitaxel, Tx soln = paclitaxel solution, 309 nm NP = nanospheres of size 309 nm, 450 nm NP = nanospheres of size 450 nm, 1µ MP = microspheres of size 1 µm, 2µ MP = microspheres of size 2 µm. (*Indicates statistically significant at α = 0.05.) Mean ± SE.

association from the smallest 309 nm particles was attributed to the unentrapped free drug present on the surface of the nanospheres. This experiment also reconfirmed that particle size did not influence the association of paclitaxel from the particles into the BBMEC monolayer.

Effect of Paclitaxel-PLGA Particle Size on 4T1 Cytotoxicity

Consistent with the data for the association of paclitaxel into 4T1 cells, the cytotoxicity of paclitaxel increased as the size of paclitaxel-PLGA particles increased. Figure 10b indicates that paclitaxel particles larger than 450 nm were more cytotoxic (p value > 0.05) than the smaller 310-nm nanospheres (Fig. 10a) or solution. The mean IC_{50} values of paclitaxel in solution and the 310-, 450-, 1040-, and 2077-nm particles were 2.06, 2.03, 0.89, 0.64, and 0.99 µM, respectively, signifying a 5-fold increase in cytotoxicity of 1-µm particles compared to the solution. The cytotoxicity of the 2-µm microspheres was lower than the 1-µm particles because from the release studies, it was observed that only 34% of the drug was released in 72 h from 2-µm particles when compared to 55% from 1 µm. This slow release from the larger particles accounted for the low cytotoxicity in 72 h. However, our subsequent *in vivo* studies for 30 days demonstrated maximum reduction of tumor with 2-µm particles. It was postulated that the increase in cytotoxicity was due to the larger microspheres adhering to the surface of the 4T1 epithelial cells, while slowly releasing paclitaxel to, or in close proximity to, the surrounding cells facilitate increased association. We conclude that nanospheres were less cytotoxic than microspheres because they did not adhere to the cell surface and were not readily internalized. No significant change in the viability of 4T1 cells was observed in the absence of paclitaxel (i.e., control).

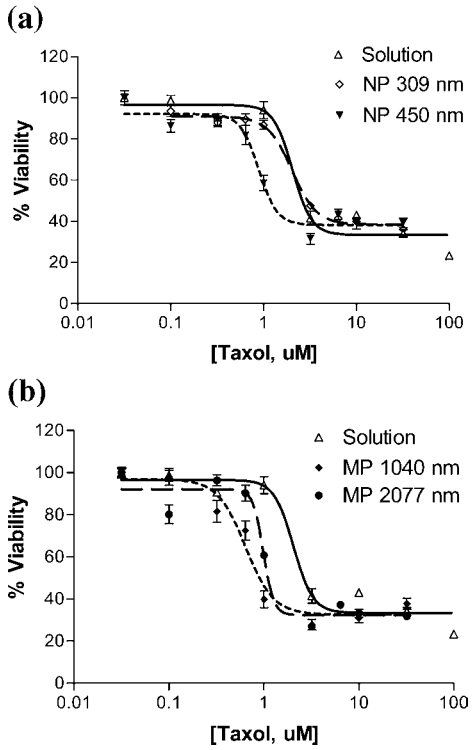

Fig. 10. Effect of particle size of nanospheres (a) and microspheres (b) on the cytotoxicity of paclitaxel in 4T1 monolayers. Solution = paclitaxel solution, NP 309 nm = nanospheres of size 309 nm, NP 450 nm = nanospheres of size 450 nm, MP 1044 nm = microspheres of size 1 µm, MP 2077 nm = microspheres of size 2 µm. Mean ± SE.

CONCLUSIONS

The effect of particle size on the cell-association and cytotoxicity of paclitaxel was tested in a murine breast cancer cell, 4T1. Contrary to literature data, the cell-association of paclitaxel into 4T1 cells increased as the particle size increased. This increase in cell-association of paclitaxel when delivered from microspheres was also observed in the cancerous, epithelial Caco-2, and Cor-L-23/R cells. Particle size of the delivery system did not influence the concentration of paclitaxel in the endothelial BBMECs. Studies with FTC, a BCRP inhibitor, indicated that the efflux pump was either absent from 4T1 cells or did not significantly inhibit the efflux of paclitaxel. In the presence of an endocytic inhibitor, 2-deoxyglycose, cell-association of PLGA particles containing paclitaxel was significantly reduced, although more drug accumulated into cells as particle size increased. This suggested that whereas nanospheres were predominantly internalized, larger microspheres may adhere to the cell surface. The adhesion of microspheres to the cell surface was nonspecific and may be due to the presence of mucus in epithelial cancer cells. Confocal microscopy supported our explanation that the increase in cell-association of paclitaxel when delivered from microspheres was due to adhesion of the particles to the cells and prolonged localized release of the drug. The increased adhesion of the microspheres to the surface of the cells could be a function of the mucin present on the surface of the epithelial cells absent from endothelial cells or the presence of high charge density on the surface of endothelial cells. Consistent with the cell-association study, there was a 5-fold decrease in the IC_{50} value of paclitaxel delivered from 1-µm microspheres compared to the drug in solution. Similar to findings with paclitaxel, the cell-association of etoposide into 4T1 cells also increased as the particle size increased. These data support the conclusion that the increased cell-association of the drug was due to the size of the delivery system and not dependent on the properties of the entrapped drug.

ACKNOWLEDGMENT

The authors thank Dr. R. Schultz, National Institutes of Health, for kindly providing Fumitremorgin-C.

REFERENCES

1. American Cancer Society Inc. Cancer Facts and Figures 2004. No. 5008.04. Available at http://www.cancer.org/downloads/STT/CAFF_finalPWSecured.pdf.
2. S. B. Horwitz, D. Cohen, S. Rao, I. Ringel, H. J. Shen, and C. P. Yang. Taxol: mechanisms of action and resistance. *J. Natl. Cancer Inst. Monogr.* **15**:55–61 (1993).
3. M. A. Jordon and L. Wilson. Microtubule polymerization dynamics, mitotic block, and cell death by paclitaxel at low concentrations. In G. I. George, T. T. Chen, I. Ojima, and D. M. Vyas (eds.), *Taxane Anti-Cancer Agents: Basic Science and Current Status*, Vol. 583, ACS Symposium Series, American Chemical Society, Washington D.C., 1995, pp. 138–153.
4. C. L. Vogel and J. M. Nabholtz. Monotherapy of metastatic breast cancer: a review of newer agents. *Oncologist* **4**:17–33 (1999).
5. A. K. Singla, A. Garg, and D. Aggarwal. Paclitaxel and its formulations. *Int. J. Pharm.* **235**:179–192 (2002).
6. R. Panchagnula. Pharmaceutical aspects of paclitaxel. *Int. J. Pharm.* **172**:1–15 (1998).
7. A. B. Dhanikula and R. Panchagnula. Localized paclitaxel delivery. *Int. J. Pharm.* **183**:85–100 (1999).
8. R. M. Straubinger and A. Sharma, U. S. Sharma, and S. V. Balasubramanian. Pharmacology and antitumor effect of novel paclitaxel formulations. In G. I. George, T. T. Chen, I. Ojima, and D. M. Vyas (eds.), *Taxane Anti-Cancer Agents: Basic Science and Current Status*, Vol. 583, ACS Symposium Series, John Wiley & Sons, Inc., Somerset, N.J. 1995, pp. 111–123.
9. N. Authier, J. P. Gillet, J. Fialip, A. Eschalier, and F. Coudore. Description of a short-term Taxol-induced nociceptive neuropathy in rats. *Brain Res.* **887**:239–249 (2000).
10. H. Gelderblom, J. Verweij, K. Nooter, and A. Sparreboom. Cremophor EL: the drawbacks and advantages of vehicle selection for drug formulation. *Eur. J. Cancer* **37**:1590–1598 (2001).
11. M. M. Amiji, P. K. Lai, D. B. Shenoy, and M. Rao. Intratumoral administration of paclitaxel in an *in situ* gelling poloxamer 407 formulation. *Pharm. Dev. Technol.* **7**:195–202 (2002).
12. J. K. Jackson, K. C. Skinner, L. Burgess, T. Sun, W. L. Hunter, and H. M. Burt. Paclitaxel-loaded crosslinked hyaluronic acid films for the prevention of postsurgical adhesions. *Pharm. Res.* **19**:411–417 (2002).
13. P. P. Constantinides, K. J. Lambert, A. K. Tustian, B. Schneider, S. Lalji, W. Ma, B. Wentzel, D. Kessler, D. Worah, and S. C. Quay. Formulation development and antitumor activity of a filter-sterilizable emulsion of paclitaxel. *Pharm. Res.* **17**:175–182 (2000).
14. P. Simamora, R. M. Dannenfelser, S. E. Tabibi, and S. H. Yalkowsky. Emulsion formulations for intravenous administration of paclitaxel. *PDA J. Pharm. Sci. Technol.* **52**:170–172 (1998).
15. P. Kan, Z. B. Chen, C. J. Lee, and I. M. Chu. Development of nonionic surfactant/phospholipid o/w emulsion as a paclitaxel delivery system. *J. Controlled Release* **58**:271–278 (1999).
16. C. Eng, A. M. Mauer, G. F. Fleming, D. Bertucci, J. Rotmensch, R. H. Jacobs, and M. J. Ratain. Phase I study of pegylated liposomal doxorubicin, paclitaxel, and cisplatin in patients with advanced solid tumors. *Ann. Oncol.* **12**:1743–1747 (2001).
17. N. V. Koshkina, J. C. Waldrep, L. E. Roberts, E. Golunski, S. Melton, and V. Knight. Paclitaxel liposome aerosol treatment induces inhibition of pulmonary metastases in murine renal carcinoma model. *Clin. Cancer Res.* **7**:3258–3262 (2001).
18. E. C. Unger, T. P. McCreery, R. H. Sweitzer, V. E. Caldwell, and Y. Wu. Acoustically active lipospheres containing paclitaxel: a new therapeutic ultrasound contrast agent. *Invest. Radiol.* **33**:886–892 (1998).
19. E. Harper, W. Dang, R. G. Lapidus, and R. I. Garver Jr. Enhanced efficacy of a novel controlled release paclitaxel formulation (PACLIMER delivery system) for local-regional therapy of lung cancer tumor nodules in mice. *Clin. Cancer Res.* **5**:4242–4248 (1999).
20. S. K. Dordunoo, J. K. Jackson, L. A. Arsenault, A. M. Oktaba, W. L. Hunter, and H. M. Burt. Taxol encapsulation in poly(epsilon-caprolactone) microspheres. *Cancer Chemother. Pharmacol.* **36**:279–282 (1995).
21. S. S. Feng, G. F. Huang, and L. Mu. Nanospheres of biodegradable polymers: a system for clinical administration of an anticancer drug paclitaxel (Taxol). *Ann. Acad. Med. Singapore* **29**:633–639 (2000).
22. H. M. Burt, J. K. Jackson, S. K. Bains, R. T. Liggins, A. M. Oktaba, A. L. Arsenault, and W. L. Hunter. Controlled delivery of taxol from microspheres composed of a blend of ethylene-vinyl acetate copolymer and poly (d,l-lactic acid). *Cancer Lett.* **88**:73–79 (1995).
23. R. Cavalli, O. Caputo, and M. R. Gasco. Preparation and characterization of solid lipid nanospheres containing paclitaxel. *Eur. J. Pharm. Sci.* **10**:305–309 (2000).
24. T. Chandy, G. H. Rao, R. F. Wilson, and G. S. Das. Development of poly(Lactic acid)/chitosan co-matrix microspheres: controlled release of taxol-heparin for preventing restenosis. *Drug Deliv.* **8**:77–86 (2001).
25. G. S. Das, G. H. R. Rao, R. F. Wilson, and T. Chandy. Controlled delivery of taxol from poly(ethylene glycol)-coated poly(lactic acid) microspheres. *J. Biomed. Mater. Res.* **55**:96–103 (2001).
26. S. Y. Kim and Y. M. Lee. Taxol-loaded block copolymer nanospheres composed of methoxy poly(ethylene glycol) and poly(epsilon-caprolactone) as novel anticancer drug carriers. *Biomaterials* **22**:1697–1704 (2001).
27. K. E. Lee, B. K. Kim, and S. H. Yuk. Biodegradable polymeric nanospheres formed by temperature-induced phase transition in a mixture of poly(lactide-co-glycolide) and poly(ethylene oxide)-poly(propylene oxide)-poly(ethylene oxide) triblock copolymer. *Biomacromolecules* **3**:1115–1119 (2002).
28. R. T. Liggins and H. M. Burt. Paclitaxel loaded poly(L-lactic acid) microspheres: properties of microspheres made with low molecular weight polymers. *Int. J. Pharm.* **222**:19–33 (2001).
29. A. Miglietta, R. Cavalli, C. Bocca, L. Gabriel, and M. R. Gasco. Cellular uptake and cytotoxicity of solid lipid nanospheres (SLN) incorporating doxorubicin or paclitaxel. *Int. J. Pharm.* **210**:61–67 (2000).
30. H. Sato, Y. M. Wang, I. Adachi, and I. Horikoshi. Pharmacokinetic study of taxol-loaded poly(lactic-co-glycolic acid) microspheres containing isopropyl myristate after targeted delivery to the lung in mice. *Biol. Pharm. Bull.* **19**:1596–1601 (1996).
31. H. Suh, B. Jeong, R. Rathi, and S. W. Kim. Regulation of smooth muscle cell proliferation using paclitaxel-loaded poly(ethylene oxide)-poly(lactide/glycolide) nanospheres. *J. Biomed. Mater. Res.* **42**:331–338 (1998).
32. Y. M. Wang, H. Sato, I. Adachi, and I. Horikoshi. Preparation and characterization of poly(lactic-co-glycolic acid) microspheres for targeted delivery of a novel anticancer agent, taxol. *Chem. Pharm. Bull. (Tokyo)* **44**:1935–1940 (1996).
33. S. Feng and G. Huang. Effects of emulsifiers on the controlled release of paclitaxel (Taxol) from nanospheres of biodegradable polymers. *J. Control. Rel.* **71**:53–69 (2001).
34. L. Mu and S. S. Feng. Fabrication, characterization and in vitro release of paclitaxel (Taxol) loaded poly (lactic-co-glycolic acid) microspheres prepared by spray drying technique with lipid/cholesterol emulsifiers. *J. Control. Rel.* **76**:239–254 (2001).
35. L. Mu and S. S. Feng. Vitamin E TPGS used as emulsifier in the solvent evaporation/extraction technique for fabrication of polymeric nanospheres for controlled release of paclitaxel (Taxol). *J. Controlled Release* **80**:129–144 (2002).
36. A. Lamprecht, U. Schafer, and C. M. Lehr. Size-dependent bioadhesion of micro- and nanoparticulate carriers to the inflamed colonic mucosa. *Pharm. Res.* **18**:788–793 (2001).
37. M. P. Desai, V. Labhasetwar, G. L. Amidon, and R. J. Levy. Gastrointestinal uptake of biodegradable microparticles: effect of particle size. *Pharm. Res.* **13**:1838–1845 (1996).
38. M. P. Desai, V. Labhasetwar, E. Walter, R. J. Levy, and G. L. Amidon. The mechanism of uptake of biodegradable microparticles in Caco-2 cells is size dependent. *Pharm. Res.* **14**:1568–1573 (1997).
39. M. Paul, R. Durand, Y. Boulard, T. Fusai, C. Fernandez, D. Rivollet, M. Deniau, and A. Astier. Physicochemical characteristics of pentamidine-loaded polymethacrylate nanoparticles: im-

plication in the intracellular drug release in Leishmania major infected mice. *J. Drug Target.* **5**:481–490 (1998).
40. J. Kunta, J. Yan, V. D. Makhey, and P. J. Sinko. Active efflux kinetics of etoposide from rabbit small intestine and colon. *Biopharm. Drug Dispos.* **21**:83–93 (2000).
41. Y. Zheng, Y. Ikuno, M. Ohj, S. Kusaka, R. Jiang, O. Cekic, M. Sawa, and Y. Tano. Platelet-derived Growth Factor Receptor Kinase Inhibitor AG1295 and Inhibition of Experimental Proliferative Vitreoretinopathy. *Jpn. J. Ophthalmol.* **47**:158–165 (2003).
42. Y. Abe, M. Ueshige, M. Takeuchi, M. Ishii, and Y. Akagawa. Cytotoxicity of antimicrobial tissue conditioners containing silver-zeolite. *Int. J. Prosthodont.* **16**:141–144 (2003).
43. L. K. Shao and D. C. Locke. Determination of paclitaxel and related taxanes in bulk drug and injectable dosage forms by reversed phase liquid chromatography. *Anal. Chem.* **69**:2008–2016 (1997).
44. J. C. Shaw, J. R. Chen, and D. Chow. Preformulation study of etoposide: identification of physicochemical characteristics responsible for the low and erratic oral bioavailability of etoposide. *Pharm. Res.* **6**:408–412 (1989).
45. L. Brannon-Peppas and J. O. Blanchette. Nanoparticle and targeted systems for cancer therapy. *Adv. Drug Deliv. Rev.* **56**:1649–1659 (2004).
46. S. De and D. H. Robinson. Particle size and temperature effect on the physical stability of plga nanospheres and microspheres containing bodipy. *AAPS PharmSciTech*. Available at **5**: http://www.aapspharmscitech.org/articles/pt0504/pt050453/pt050453.pdf (2004).
47. M. Ravi Kumar, G. Hellermann, R. F. Lockey, and S. S. Mohapatra. Nanoparticle-mediated gene delivery: state of the art. *Expert Opin. Biol. Ther.* **4**:1213–1224 (2004).
48. L. Bonhomme-Faivre, A. Pelloquin, S. Tardivel, S. Urien, M. C. Mathieu, V. Castagne, B. Lacour, and R. Farinotti. Recombinant interleukin-2 treatment decreases P-glycoprotein activity and paclitaxel metabolism in mice. *Anticancer Drugs* **13**:51–57 (2002).
49. R. V. Kondratov, P. G. Komarov, Y. Becker, A. Ewenson, and A. V. Gudkov. Small molecules that dramatically alter multidrug resistance phenotype by modulating the substrate specificity of P-glycoprotein. *Proc. Natl. Acad. Sci. USA* **98**:14078–14083 (2001).
50. H. Burger, H. van Tol, A. W. Boersma, M. Brok, E. A. Wiemer, G. Stoter, and K. Nooter. Imatinib mesylate (STI571) is a substrate for the breast cancer resistance protein (BCRP)/ABCG2 drug pump. *Blood* **104**:2940–2942 (2004).
51. A. Suvannasankha, H. Minderman, L. O'Loughlin, T. Nakanishi, L. A. Ford, W. R. Greco, M. Wetzler, D. D. Ross, and M. R. Baer. Breast cancer resistance protein (BCRP/MXR/ABCG2) in adult acute lymphoblastic leukaemia: frequent expression and possible correlation with shorter disease-free survival. *Br. J. Haematol.* **127**:392–398 (2004).
52. X. Wang, T. Nitanda, M. Shi, M. Okamoto, T. Furukawa, Y. Sugimoto, S. Akiyama, and M. Baba. Induction of cellular resistance to nucleoside reverse transcriptase inhibitors by the wild-type breast cancer resistance protein. *Biochem. Pharmacol.* **68**:1363–1370 (2004).
53. V. Vasilevko, A. Ghochikyan, N. Sadzikava, I. Petrushina, M. Tran, E. P. Cohen, P. J. Kesslak, D. H. Cribbs, G. L. Nicolson, and M. G. Agadjanyan. Immunization with a vaccine that combines the expression of MUC1 and B7 co-stimulatory molecules prolongs the survival of mice and delays the appearance of mouse mammary tumors. *Clin. Exp. Metastasis* **20**:489–498 (2003).
54. J. E. Eyles, Z. C. Carpenter, H. O. Alpar, and E. D. Williamson. Immunological aspects of polymer microsphere vaccine delivery systems. *J. Drug Target.* **11**:509–514 (2003).
55. G. Vassiliou and R. McPherson. Role of cholesteryl ester transfer protein in selective uptake of high density lipoprotein cholesteryl esters by adipocytes. *J. Lipid Res.* **45**:1683–1693 (2004).
56. J. S. Popova and M. M. Rasenick. Clathrin-mediated endocytosis of m3 muscarinic receptors. Roles for Gbetagamma and tubulin. *J. Biol. Chem.* **279**:30410–30418 (2004).
57. D. W. Miller, B. T. Keller, and R. T. Borchardt. Identification and distribution of insulin receptors on cultured bovine brain microvessel endothelial cells: possible function in insulin processing in the blood-brain barrier. *J. Cell. Physiol.* **161**:333–341 (1994).
58. W. Liang, M. Buluc, C. van Breemen, and X. Wang. Vectorial Ca2+ release via ryanodine receptors contributes to Ca2+ extrusion from freshly isolated rabbit aortic endothelial cells. *Cell Calcium* **36**:431–443 (2004).
59. F. F. Vargas, M. H. Osorio. U. S. Ryan, and M. De Jesus. Surface charge of endothelial cells estimated from electrophoretic mobility. *Membr. Biochem.* **8**:221–227 (1989).